ADVANCED MATERIALS

[9] A. K. Hebb, K. Senoo, R. Bhat, A. I. Cooper, *Chem. Mater.* **2003**, *15*, 2061.
[10] G. Maier, *Prog. Polym. Sci.* **2001**, *26*, 3.
[11] J. Lee, A. Hirao, S. Nakahama, *Macromolecules* **1998**, *21*, 274.
[12] V. Z-H. Chan, J. Hoffman, V. Y Lee, H. Iatrou, A. Avgeropoulos, N. Hadjichristidis, R. D. Miller, E. L. Thomas, *Science* **1999**, *286*, 1716.
[13] A. S. Zalusky, R. Olayo-Valles, A. H. Wolf, M. A. Hillmyer, *J. Am. Chem. Soc.* **2002**, *124*, 12761.
[14] T. Hashimoto, K. Tsutsumi, Y. Funaki, *Langmuir* **1997**, *13*, 6869.
[15] K. Sugiyama, T. Nemoto, G. Koide, A. Hirao, *Macromol. Symp.* **2002**, *181*, 135.
[16] M. L. O'Neill, Q. Cao, M. Fang, K. P. Johnston, S. P. Wilkinson, C. D. Smith, J. L. Kerschner, S. H. Jureller, *Ind. Eng. Chem. Res.* **1998**, *37*, 3067.
[17] C. Harrison, M. Park, P. Chaikin, R. A. Register, D. H. Adamson, N. Yao, *Macromolecules* **1998**, *31*, 2185.
[18] H. Yokoyama, T. E. Mates, E. J. Kramer, *Macromolecules* **2000**, *33*, 1888.
[19] W. V. Wang, E. J. Kramer, W. H. Sachse, *J. Polym. Sci., Polym. Phys. Ed.* **1982**, *20*, 1371.
[20] S. K. Goel, E. J. Beckman, *Polymer* **1993**, *34*, 1410.
[21] T. A. Walker, S. R. Raghavan, J. R. Royer, S. D. Smith, G. D. Wignall, Y. Melnichenko, S. A. Khan, R. J. Spontak, *J. Phys. Chem. B* **1999**, *103*, 5472.
[22] M. Born, E. Wolf, in *Principles of Optics*, Cambridge University Press, Cambridge, UK **1999**.

A Microporous Titania Membrane for Nanofiltration and Pervaporation**

By *Jelena Sekulić*, *Johan E. ten Elshof*,* and *Dave H. A. Blank*

Ceramic microporous membranes with pore sizes < 2 nm are known for their relatively high chemical, mechanical, and thermal stability, and they offer potential applications in gas purification and separation, pervaporation, and nanofiltration processes. However, very few microporous ceramic materials with a pore size < 1 nm (therefore suitable for membrane applications) are available. Amorphous silica membranes with pore sizes of between 0.3–0.5 nm have been studied extensively over the past decade.[1] However, ceramic sol–gel membranes with a narrow pore size distribution and pore sizes in the range of 0.6–1.3 nm are scarce.[2] Although microporous silica is a very selective membrane material for hydrogen separation[3] and pervaporation of water from liquid mixtures,[4] its chemical stability in alkaline media and strong electrolyte solutions is limited.[5] The amorphous phase of titania, which is known to be microporous, is expected to be more stable under these conditions. We prepared defect-free microporous titania membranes of between 50–150 nm thickness with a maximum pore size of ~0.9 nm. These membranes demonstrated ideal hydrogen/hydrocarbon permselectivities above the theoretical limit for Knudsen diffusion and have also been shown to be selective in the pervaporation of water from water/1,4-dioxane and water/glycol binary liquids. Moreover, nanofiltration experiments have showed that these membranes have a molecular weight cut-off below 400, indicating their potential for water purification applications.

Attempts in the 1990s to prepare microporous titania membranes already showed some promising results, but the average pore sizes obtained in those studies were ~1.5 nm, and the Knudsen diffusion limit was not exceeded.[6] More recently, microporous titania membranes attracted attention as nanofiltration membranes[7] and molecular weight cut-offs ranging between 500–600 were reported.

We studied the relationship between sol–gel processing conditions and the titania microstructure. Polymeric titania sols in ethanol were prepared by mixing titanium alkoxide solutions with water and nitric acid. Unlike silica, which does not crystallize, amorphous titania easily converts into crystalline anatase during synthesis. Low molecular weight polymeric sols were obtained only when the hydrolysis conditions were strictly controlled. The rate of hydrolysis of titanium alkoxides by water is extremely high[8] and any local excess of water at any moment had to be avoided. For a given titanium concentration, the hydrolysis-condensation reactions were governed by two parameters, the initial hydrolysis ratio $r_w = [H_2O]/[Ti]$ and the inhibitor ratio $r_a = [H^+]/[Ti]$. The hydrolysis of titanium tetraethoxide in the presence of different amounts of acid and water led to sols, turbid or clear gels, or precipitates, depending on r_w and r_a, as shown in Figure 1a. The main determining parameter for the final particle size was found to be r_w, which had to be kept at values below 2 in order to prevent fast gelation of the sol. A pH > 3 solution was required to form polymeric sols, and these were stable for at least several months.

The average sol particle size was determined by light scattering and small angle X-ray scattering (SAXS), while the latter method also provided information about the polymeric structure of the sols.[9] A SAXS curve of a stable amorphous titania sol with $r_w = 1.7$ is shown in Figure 1b. Since the titania sols are polymeric by nature, their scattering curve could be fitted to the Teixeira function,[10] which describes the scattering curve of fractal objects. This provided three parameters, namely the radius of the individual scatterer R_0, the correlation length of self-similar behavior of the sol particles ξ, and the fractal dimension of the particles D_f. The value of R_0 should be roughly equal to the Ti-O monomer bond length of ~0.19 nm, and ξ can be related to the Guinier radius of the in-

[*] Dr. J. E. ten Elshof, Dr. J. Sekulic
Prof. D. H. A. Blank
Department of Science and Technology
MESA+ Institute for Nanotechnology, Inorganic Materials Science
University of Twente
P.O. Box 217, NL-7500 AE, Enschede (The Netherlands)
E-mail: j.e.tenelshof@utwente.nl

[**] Part of this work was financially supported by the European Communities in the framework of the Growth Programme, contract no. G1RD-CT-1999-00076. Prof. A. van Veen and R. Escobar Galindo are gratefully acknowledged for the positron annihilation experiments.

  DOI: 10.1002/adma.200306472

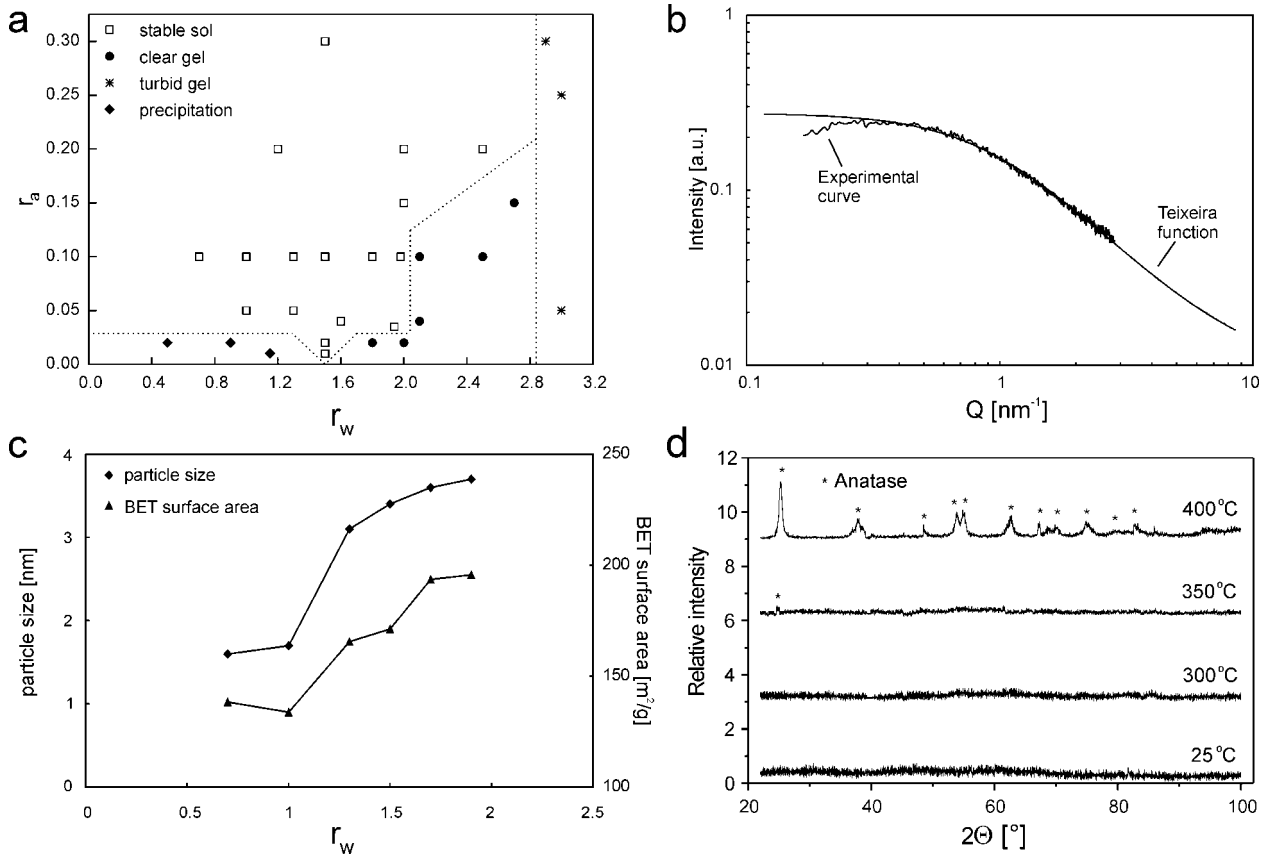

Figure 1. a) Pseudo-phase diagram of polymeric titania sol showing influence of hydrolysis (r_w) and inhibition (r_a) ratios on sol state. b) Small angle x-ray scattering curve of titania sol ($r_w = 1.7$) and best fit of the Teixeira function to the experimental data. c) d) Sol particle sizes versus r_w after 24 h ageing as determined by light scattering at $r_a = 0.15$. d) Temperature programmed XRD spectra of titania.

organic polymer R_g via $R_g^2 = \frac{1}{2} D_f (D_f + 1) \xi^2$. The fractal dimension D_f is related to the mass m and radius r of the sol particle via $m \propto r^{D_f}$. D_f has an upper limiting value of 3, where the object is Euclidean. As D_f decreases, the object will look sparser, giving essentially a linear object when $D_f = 1$. The best fits were obtained with $R_0 \sim 0.2$ nm, $\xi \sim 1.1$–1.4, and $D_f \sim 1.5$–1.7. This corresponds with a radius of gyration R_g between 1.7 and 1.9 nm, or an average particle size of 3.4–3.8 nm. This value is very similar to the size of 3.6 nm that was measured by light scattering as shown in Figure 1c. Larger r_w values gave rise to larger sol particles, but also to larger Brunauer–Emmett–Teller (BET) surface areas in the final calcined powders, which indicates that the overall porosity increased and the pore size decreased with r_w. The increase of BET surface area with increasing particle diameter suggests that the microporous titania powder has a polymeric microstructure, because the trend would have been opposite if the primary particles had been colloidal in nature. Further information regarding the microstructure of the final membrane layer is provided by the value D_f. As the tendency of two fractal particles m_1 and m_2 with dimension D_f to interpenetrate is inversely related to the number of intersections, the relationship between two merged particles $m_{12} = m_1 + m_2$ can be described as $m_{12} \propto r^{2D_f - 3}$.[11] This indicates that dense packing of particles is only possible when $D_f < 1.5$. The amorphous titania sols have a slightly higher value of ~1.6, which suggests that very dense packing and a very high degree of interpenetration as occurs for microporous silica[9] will not occur. Hence the average pore size of titania powders and membranes is expected to be larger than for silica.

Amorphous titania was found to be chemically stable in water between pH values of 1–13, while significant dissolution occurred at lower pH values. This is a considerable improvement in comparison with microporous silica, which dissolves at values > pH 9.[5] The thermal evolution of microstructure was recorded by temperature programmed X-ray diffraction (XRD) spectra. The results are displayed in Figure 1d. The amorphous structure was retained in air until 300–350 °C. At 400 °C a partial phase transformation into crystalline anatase occurred, and this was accompanied by a microstructural collapse.

Highly reproducible, homogeneous and crack-free microporous amorphous titania layers were prepared on mesoporous γ-alumina coated α-alumina substrates. The layer thickness

ADVANCED MATERIALS

could be varied between ~30 nm and ~1 μm by changing the sol concentration prior to the layer deposition. After heat treatment, the Kelvin radius of all pores was below the experimental lower limit of ~1.7 nm of the permporometry method. An example of a supported amorphous titania membrane is shown on the scanning electron microscope (SEM) image in Figure 2a.

The supported membranes were further characterized with positron beam analysis (PBA) and reflectivity measurements, which have the advantage of being non-destructive methods. PBA is based on a positron (e^+) "interaction" with a material. Several modes of operation are used to obtain information about the composition and microstructure of a material: Doppler broadening of annihilation radiation (DBAR), two-dimensional angular correlation of annihilation radiation (2D-ACAR), and positron annihilation lifetime analysis.[12] The positron implantation energy is a measure of the depth inside the material that is being probed. DBAR measurements can be interpreted in terms of two parameters. The *S* (shape) parameter, defined as the ratio of the central part of the annihilation spectrum and the total spectrum, reflects positron annihilation with low momentum valence electrons. In general, a high value of *S* indicates positron annihilation in open volume defects, and is therefore a measure of porosity. The second parameter is the *W* (wing) parameter, which reflects positron annihilation with high momentum electrons (core electrons), and is therefore related to the chemical environment where the annihilation takes place. The PBA results are shown in Figure 2b. The ~80 nm thick titania top layer, ~550 nm thick γ-alumina intermediate layer, and part of the α-alumina support structure are indicated in the figure. In terms of positron annihilation, the formation of positronium (a hydrogen-like quantum-mechanical particle of ~1 nm size that consists of a positron–electron (e^+,e^-) pair) in a layer indicates a percolative pore structure with pore size >1 nm.[12] As shown in the figure, the positronium fraction in the titania top layer was very low, which strongly suggests that the pore size in this layer was smaller than 1 nm, thus making it impossible for a positronium to form. In contrast, a high fraction of positronium was formed in the underlying γ-alumina layer, which is known to have a percolative pore structure with pore sizes in the range of 4.5–7 nm.[13] The *S* parameter in the titania layer was found to have values in between that of γ-alumina (55 % porosity) and α-alumina (30 % porosity). This agreed well with the porosity of 35–40 % as calculated from reflectivity measurements on titania layers, and both values are close to the ~37 % residual porosity in a system of randomly close-packed dense spherical particles.[14] The *W* parameter varied little over the different layers due to their oxidic nature.

The small pore size of titania was further confirmed by the series of transport measurements, that could be an indication for the possible membrane applications. Nanofiltration tests were carried out with solutions containing ethylene glycol based compounds with molecular weights ranging between 60–400 g mol^{-1}. As can be seen in Figure 3a, the retention of ethylene glycol molecules increased with molecular size, and exceeded a value of 90 % for polyethylene glycol (PEG), $M_w = 400$ g mol^{-1}. Since the Stokes radius a (Å) of PEG with a molecular weight M (g mol^{-1}) is given by $a \approx 0.17\ M^{0.557}$,[15] it can be estimated that the maximum pore diameter is ~0.9 nm or smaller. Although the molecular weight cut-off measurements can only give a rough estimate of the membrane pore size, the result is in qualitative agreement with the observations of the reflectivity and positron annihilation measurements, and confirms the successful formation of a stable, defect-free titania membrane with pore size in a sub-nanometer range.

Single gas permeation measurements were carried out in order to obtain information on the dominant mechanism of gas transport.[1] The permeances *F*, i.e., the molar gas flux per unit driving force, of several gases are shown in Figure 3b. The permeance of microporous silica calcined at 400 °C is shown

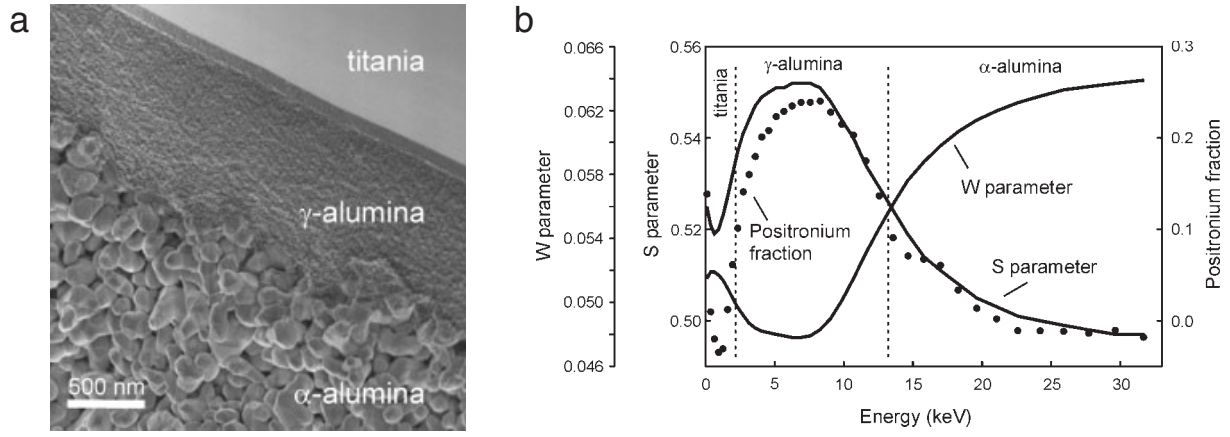

Figure 2. a) SEM picture of a cross-section of a 100 nm thick amorphous TiO_2 layer on a γ-Al_2O_3 coated α-Al_2O_3 substrate. b) Positronium fraction, and *S* and *W* parameters from Positron Beam Analysis experiments as a function of positron implantation energy. The implantation energy is related to depth inside the membrane.

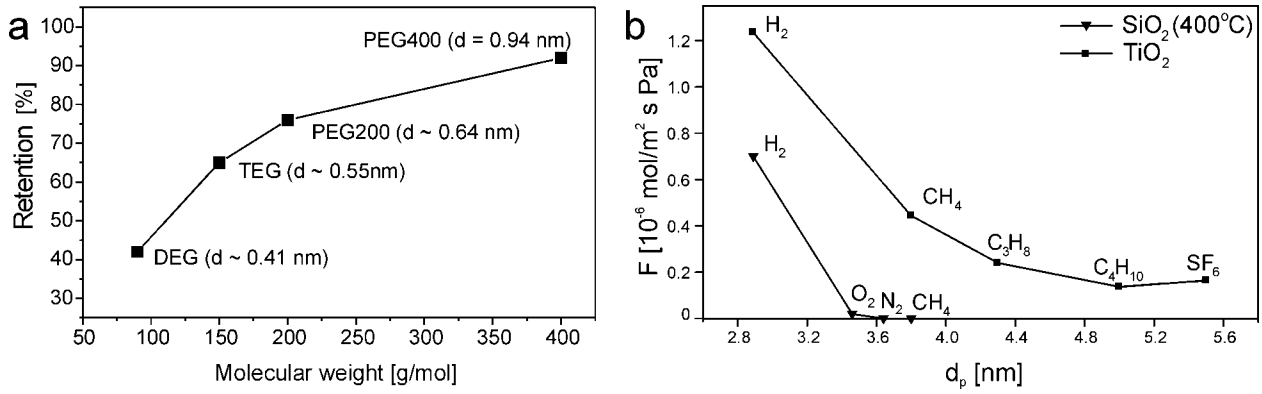

Figure 3. a) Retention of microporous titania membrane towards small molecules in nanofiltration experiments. b) Single gas permeances *F* of gases with kinetic diameter d_p through a 100 nm thick microporous titania membrane at 200 °C and comparison with 400 °C-calcined microporous silica.

for comparison. Clearly, microporous titania allows diffusion of larger molecules than silica, which indicates the presence of large pores than in silica. The ideal $H_2/n\text{-}C_4H_{10}$ permselectivity, defined as the ratio of single gas permeances, was 9–12, while the theoretical upper limit for Knudsen diffusion was ~5.4. With the exception of SF_6 the ideal permselectivities F_{H_2}/F_{CxHy} of all gases exceeded the theoretical upper limit for Knudsen-type (mesopore) diffusion.[2] This indicates that micropore diffusion plays a dominant role in the gas transport through this membrane.

Microporous titania membranes also showed selective pervaporation of water from 8–13 wt.-% water/1,4-dioxane mixtures at 80 °C. Separation factors of ~4 were obtained with accompanying fluxes of 2.7–2.8 $kg\,m^{-2}\,h^{-1}$. Pervaporation experiments with molecules smaller than 1,4-dioxane, which has an estimated molecular diameter of ~0.7 nm,[4a] did not show any selective pervaporation. This suggests that the selectivity was at least partly due to a molecular sieving effect, i.e., the pore size of titania appears to play a definite role in achieving selectivity in this process. Separation factors of over 100 were achieved for water/glycol mixtures with 2–5 wt.-% water in the feed, at temperatures >80 °C. Low water fluxes of ~0.2 $kg\,m^{-2}\,h^{-1}$ were measured. The relatively large dipole moment of ethylene glycol (2.28 D) and its ability to form hydrogen bonds probably lead to strong attractive interactions within the internal titania surface. Ethylene glycol molecules are probably small enough to enter the titania pores, but they will diffuse slowly, thereby blocking the channels for further ethylene glycol transport, and retarding the transport of water.

In conclusion, a microporous titania-based molecular sieving membrane with high potential for nanofiltration and pervaporation processes was prepared by the polymeric sol–gel method. These membranes were chemically stable in a wide pH range. Strict control of the reaction parameters is an important consideration when dealing with small nanoparticles which possess a low fractal dimension. These structures furnish membranes with an active pore size of ~0.9 nm and an accompanying molecular sieving ability.

Experimental

Sol Preparation: Polymeric titania sols were prepared by mixing two separate solutions in an appropriate ratio in a dry nitrogen atmosphere under vigorous stirring. Solution 1 contained a solution of titanium tetraethoxide (Aldrich) in dehydrated ethanol. Solution 2 consisted of nitric acid (65 % solution, Merck) and Q2 water in ethanol. The sol was stabilized by refluxing at 60 °C for 10 mins, followed by aging at room temperature for at least 24 h.

Film Formation: Titania sols were deposited on flat mesoporous γ-alumina coated α-alumina disks of 39 mm diameter by standard dip coating techniques. To avoid crystallization of amorphous titania upon too fast drying, the films were dried in a water-free alcohol-saturated atmosphere at room temperature for a period of 48 h. After drying the membranes were calcined in air at 300 °C for 3 h. The absence of cracks or mesopores was checked by permporometry [16].

Characterization: Temperature programmed X-ray diffraction (XRD) experiments on dried uncalcined powder and small angle X-ray scattering experiments (SAXS) on titania sols were carried out with a Philips SR5056 with Cu Kα radiation (PanAlytical, The Netherlands). The titania particle sizes in the sols were estimated using a ZetaSizer (Malvern, UK) with a lower limit for accurate detection at ~2 nm. BET measurements (Micromiretics) were performed at 77 K using N_2 as the condensable gas. The thickness and quality of the layers were checked with a high-resolution scanning electron microscope (LEO Gemini 1550 FEG-SEM, UK). Reflectometry measurements were performed on a high-resolution 4-circle diffractometer (Philips).

Positron beam analysis experiments were performed using the Doppler Broadening of Annihilation Radiation (DBAR) technique with the Delft Variable Positron Beam [12]. Positrons were injected into the membranes with energies tuned between 100 eV and 30 keV, which corresponds to a maximum penetration depth of ~2 μm in ceramics of 2.5 $g\,cm^{-3}$ density and ~5 μm in ceramics of 1 $g\,cm^{-3}$ density. The chemical stability of calcined amorphous titania and silica powders at pH 1–13 was determined at room temperature by static solubility tests in water [5]. One gram of powder was immersed in 50 mL of water. The pH of the solutions was adjusted with nitric acid or ammonium hydroxide and the total weight loss after 120 h immersion was calculated by measuring the concentration of dissolved titanium in the solution using atomic absorption spectroscopy (Thermo-Optec BV SOLAAR system 939).

Transport Experiments: Nanofiltration experiments were carried out in a pressurized dead-end filtration cell [13]. The retention of ethylene glycol based molecules was measured to determine the molecular weight cut-off (MWCO) of the membrane. Aqueous solutions containing 1 wt.-% of PEG were filtered through the membrane at pressure of 10 bar, and the retention was determined from the solute

ADVANCED MATERIALS

concentrations in the permeate solution. Single gas permeation experiments were performed at 200 °C in a cross-flow gas permeation setup [3a]. Pervaporation experiments were performed with water/1,4-dioxane and water/glycol binary liquids at 75–80 °C in a dead-end pervaporation unit [4a,5]. The permeate composition was analyzed by Karl Fischer titration.

Received: November 14, 2003
Final version: May 4, 2004

[1] a) R. J. R. Uhlhorn, M. H. B. J. Huis in 't Veld, K. Keizer, A. J. Burggraaf, *J. Mater. Sci. Lett.* **1989**, *8*, 1135. b) R. S. A. de Lange, J. H. A. Hekkink, K. Keizer, A. J. Burggraaf, *J. Membr. Sci.* **1995**, *99*, 57. c) B. N. Nair, K. Keizer, T. Okubo, S. I. Nakao, *Adv. Mater.* **1998**, *10*, 249.

[2] A. J. Burggraaf, in *Fundamentals of Inorganic Membrane Science and Technology* (Eds: A. J. Burggraaf, L. Cot), Elsevier, Amsterdam, the Netherlands **1996**, 1–35 and 331–433.

[3] a) R. M. de Vos, H. Verweij, *Science* **1998**, *279*, 1710. b) B. N. Nair, K. Keizer, H. Suematsu, Y. Suma, N. Kaneko, S. Ono, T. Okubo, S. I. Nakao, *Langmuir* **2000**, *16*, 4558.

[4] a) J. E. ten Elshof, C. Rubio Abadal, J. Sekulic, S. Roy Chowdhury, D. H. A. Blank, *Microporous Mesoporous Mater.* **2003**, *65*, 197. b) H. M. van Veen, Y. C. van Delft, C. W. R. Engelen, P. P. A. C. Pex, *Sep. Purif. Technol.* **2001**, *22–23*, 361.

[5] J. Sekulic, M. W. J. Luiten, J. E. ten Elshof, N. E. Benes, K. Keizer, *Desalination* **2002**, *148*, 19.

[6] a) Q. Xu, M. A. Anderson, *J. Am. Ceram. Soc.* **1994**, *77*, 1939. b) R. A. Peterson, M. A. Anderson, C. G. Hill, Jr., *J. Membr. Sci.* **1994**, *94*, 103.

[7] a) P. Puhlfürss, A. Voigt, R. Weber, M. Morbé, *J. Membr. Sci.* **2000**, *174*, 123. b) T. Van Gestel, C. Vandecasteele, A. Buekenhoudt, C. Dotremont, J. Luyten, R. Leysen, B. Van der Bruggen, G. Maes, *J. Membr. Sci.* **2002**, *207*, 73. c) T. Van Gestel, C. Vandecasteele, A. Buekenhoudt, C. Dotremont, J. Luyten, R. Leysen, B. Van der Bruggen, G. Maes, *J. Membr. Sci.* **2002**, *209*, 379.

[8] A. Soloviev, R. Tufeu, C. Sanchez, A. V. Kanaev, *J. Phys. Chem. B* **2001**, *105*, 4175.

[9] N. Maene, B. N. Nair, P. D'Hooghe, S. I. Nakao, K. Keizer, *J. Sol-Gel Sci. Technol.* **1998**, *12*, 117.

[10] J. Teixeira, in *On growth and form* (Eds: H. E. Stanley, N. Ostrowsky), Martinus Nijhof, Dordrecht, The Netherlands **1986**, 145–162.

[11] B. B. Mandelbrot, *The Fractal Geometry of Nature*, Freeman, San Fransisco, CA **1983**.

[12] a) A. van Veen, *J. Trace Microprobe Tech.* **1990**, *8*, 1. b) A. van Veen, H. Schut, J. de Vries, R. A. Hakfoort, M. R. IJpma, in *Positron Beams for Solids and Surfaces* (Eds: P. J. Schultz, G. R. Massoumi, P. J. Simpson), American Institute of Physics, New York **1990**, 171–196. c) A. van Veen, H. Schut, P. E. Mijnarends, in *Positron Beams and their Applications* (Ed: P. G. Coleman), World Scientific Publishing, Singapore **2000**, Ch. 6.

[13] S. Roy Chowdhury, R. Schmuhl, K. Keizer, J. E. ten Elshof, D. H. A. Blank, *J. Membr. Sci.* **2003**, *225*, 177.

[14] S. Torquato, T. M. Truskett, P. G. Debenedetti, *Phys. Rev. Lett.* **2000**, *84*, 2064.

[15] S. Singh, K. C. Khulbe, T. Ramamurthy, P. Matsuura, *J. Membr. Sci.* **1998**, *142*, 111.

[16] a) C. Eyraud, M. Betemps, J. F. Quinson, F. Chatelut, M. Brun, B. Rasneur, *Bull. Soc. Chim. Fr.* **1984**, *9–10*, I-237. b) G. Z. Cao, J. Meijerink, H. W. Brinkman, A. J. Burggraaf, *J. Membr. Sci.* **1993**, *83*, 221.

Uniform Metal Nanotube Arrays by Multistep Template Replication and Electrodeposition**

By *Cheng Mu*, *Yuxiang Yu*, *Rongming Wang*, *Kai Wu*, *Dongsheng Xu*,* and *Guolin Guo*

Since the discovery of carbon nanotubes,[1] hollow nanotubes have attracted considerable attention due to their fundamental significance and potential applications in nanoscale devices, sensors, and energy storage/conversion.[2–13] In particular, metal nanotubes raise special interest because of their conductivity, catalysis, and the feasibility of chemically modifying their outer/inner surfaces and edges. For example, gold nanotube membranes have unfolded potential applications in nanoelectrode ensembles, sensors, chemical and biological separations, and biocatalysis.[14]

To date, only a few examples of metal nanotubes have been reported in the literature.[14–19] Template-based techniques have been employed to prepare aligned metal nanotube arrays such as gold,[14] cobalt,[15] iron,[15] and nickel,[16] where the inner surfaces of the template pores need to be chemically modified prior to deposition. Xia and co-workers have synthesized noble metal nanotubes such as gold, palladium, and platinum via galvanic displacement reactions between silver or selenium nanowires and appropriate precursors of these metals in aqueous media.[17] Bismuth and antimony nanotubes have been obtained by low-temperature solvothermal methods.[18,19] However, a general approach for fabricating aligned metal nanotube arrays is still elusive. Precise control of the nanotube growth process and formation of well-aligned arrays will be of great help in investigating their physical properties and their potential use in nanoscale fluidic chemical and biological separations, sensors, and catalysis. In this work, we design a well-controlled process for fabricating uniform metal nanotube arrays via a multistep template replication and electrodeposition approach. The obtained nanotubes are highly ordered and uniform in wall thickness and diameter along the entire tubes.

[*] Prof. D. S. Xu, C. Mu, Y. X. Yu, Prof. K. Wu,
Prof. G. L. Guo
State Key Laboratory for Structural Chemistry of Unstable and Stable Species, College of Chemistry and Molecular Engineering,
Peking University
Beijing 100 871 (P.R. China)
E-mail: dsxu@chem.pku.edu.cn
Prof. R. M. Wang
Electron Microscopy Laboratory and State Key Laboratory for Mesoscopic Physics, School of Physics
Peking University
Beijing 100 871 (P.R. China)

[**] This work was supported by the Major State Basic Research Development Program (Grant No. 2000077503) from the Ministry of Science and Technology, China and KW is grateful for financial support from the NSFC (Grant No. 20125309).

  DOI: 10.1002/adma.200400129